J. Fluid Mech. (1996), *vol.* 306, *pp.* 145–165

The transitional regime between coalescing and splashing drops

By MARTIN REIN†

Max-Planck-Institut für Strömungsforschung, Bunsenstraße 10, 37073 Göttingen, Germany

(Received 29 November 1994 and in revised form 22 August 1995)

A drop that falls into a deep liquid can either coalesce with the receiving liquid and form a vortex ring or splash. Which phenomenon actually occurs depends on the impact conditions. When the impact conditions are gradually changed the transition between coalescence and splashing proceeds via a number of intermediate steps. These are studied by means of high-speed photography of the normal impact of water drops on a plane water surface. The characteristics of different flows that appear in the transitional regime and possible mechanisms causing these flows are discussed in detail. The phenomena considered include the rise of thick jets and the ejection of high-rising thin jets out of the impact crater, the entrainment of gas bubbles, crater dynamics, crown formation and the generation of splash droplets. Finally, a classification of the phenomena characteristic of the transitional regime is given.

1. Introduction

When a drop impinges on the surface of a deep liquid it either quietly coalesces with the receiving liquid or splashes. Both phenomena were studied in the last century but the transition between them was not considered until recently. Thompson & Newall (1885) examined the properties of vortex rings typically formed in the receiving liquid after coalescence. Worthington (1897) employed the new technique of short-exposure photography to resolve details during the splash of drops. In addition to splashing and coalescence, impinging drops may also bounce off or float on the liquid surface. Furthermore, gas bubbles can be entrained into the receiving liquid by several mechanisms. We have recently reviewed these and other phenomena of drop impact (Rein 1993, 1995*a*). There it was shown that in previous works different phenomena of drop impact were normally considered separately on their own and often the exact conditions of their occurrence are not well known. An exception may be the transition from coalescence to splashing which happens with increasingly energetic impacts. Near the transition to splashing another phenomenon, the so-called regular entrainment of a gas bubble, can be found. Regular entrainment appears to be connected with the formation of a narrow high-rising liquid jet as was pointed out in Rein (1993). These phenomena have been the subject of several investigations but were not related to one another. The aim of this paper is to provide a global picture of different types of fluid flow in the transitional regime between coalescence and splashing, and to describe relationships between them. In order to accomplish this we have taken high-speed photographs of drop impacts occurring under different conditions. Most previous experiments concerning these phenomena were conducted with water which was also used in the present work. Thus, both the drop and the receiving liquid are the same.

† Present address: DLR, Institut für Strömungsmechanik, Bunsenstraße 10, 37073 Göttingen, Germany.

Coalescence is usually connected with the formation of a vortex ring that propagates into the receiving liquid. Immediately after impact a crater is formed and the drop liquid spreads over its floor. The crater eventually recedes and a vortex ring appears. The surface of the receiving liquid quickly assumes its horizontal equilibrium position and is not otherwise disturbed. In particular, secondary droplets are not normally formed. In the case of splashing a deep crater is produced in the receiving liquid after impact. At its rim a crown-like cylindrical liquid film is ejected out of the crater. Small droplets are normally shed from this film. Later, when the crater collapses a liquid column rises out of its centre. The upper part of this central jet consists mainly of drop liquid. Instabilities usually cause the separation of one or more droplets from the tip of the jet. When a tip droplet later falls back into the liquid it usually coalesces and a vortex ring is formed.

Which of the features described in the last paragraph is most characteristic of coalescence and splashing, respectively, so that it may serve as a criterion for either of these phenomena? Normally, the sighting of a central jet is taken as a decision criterion for splashing. When no jet appears the impact is classified as coalescence (except for floating and bouncing drops). In contrast to this, splashing on solid walls is characterized by the formation of secondary droplets as is implied by the term *splash* (Rein 1993). During drop impact into deep liquids, however, secondary droplets need not necessarily be produced when a central jet appears. It will be shown that the formation of a jet without the shedding of secondary droplets is found only close to the splashing threshold given in terms of the jet criterion. Furthermore, either a central jet or a vortex ring will occur but not both of them. The jet criterion thus distinguishes between the two main characteristic features of drop impact into liquids. Using mainly data of Rodriguez & Mesler (1985), Hsiao, Lichter & Quintero (1988) found that drops splash when the Weber number exceeds a threshold which is a function of the Froude number. These numbers are defined by $We = \rho u^2 D/\sigma$ and $Fr = u^2/gD$, respectively, where u is the impact velocity, g the acceleration due to gravity, D the drop diameter, and ρ and σ are the density and surface tension of the liquid. Data points corresponding to the boundary between splashing and coalescence are plotted in a Weber versus Froude number diagram in figure 1 as solid circles. The splashing threshold is a nearly linear function of the Froude number.

Under certain conditions the impact of a drop on a deep liquid results in the entrainment of a single gas bubble (Pumphrey & Walton 1988). The bubble is pinched off at the bottom of the crater during the process of crater collapse. This is called regular entrainment. The oscillating bubble emits sound, which was found to be a main source of underwater noise of rain (Prosperetti, Pumphrey & Crum 1989). The conditions under which a bubble is entrained in this manner can be represented by a region of regular entrainment in a Weber versus Froude number diagram (Pumphrey & Elmore 1990). Figure 1 shows curve fits to experimental data representing the upper and lower bound of this region, We_u and We_l. Here, we have used the relations given by Oğuz & Prosperetti (1990): $We_u = 48.3\,Fr^{0.247}$ and $We_l = 41.3\,Fr^{0.179}$. The lower bound lies just above the splashing threshold, i.e. regular bubble entrainment can be considered as a special case of splashing.

Another feature observed along with drop impact is the formation of high-rising and narrow central jets when the impact velocity lies within a certain range. This phenomenon was found by Hallett & Christensen (1984) who determined the dependence on the impact velocity of the maximum height to which the central jet rises when water drops of constant radius splash on a deep liquid. They reported the existence of a small range of impact velocities where the jet height reaches a

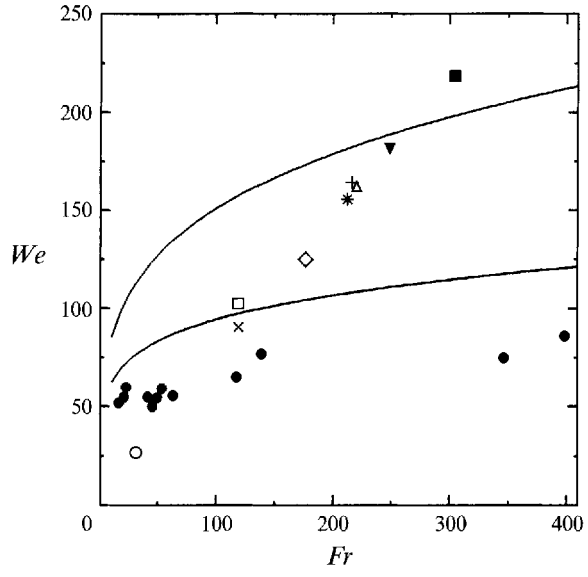

FIGURE 1. Drop impact on a deep liquid: transitional regime between coalescing and splashing drops in a Weber versus Froude number diagram. Known boundaries between regions characteristic of different phenomena are shown. Solid circles: upper boundary of vortex ring formation (data taken from Rodriguez & Mesler 1985), above this boundary a central jet is formed. Solid lines: lower and upper boundary of the region of regular bubble entrainment (data of Pumphrey & Crum, cf. Oğuz & Prosperetti 1990). The specific conditions of drop impacts that are considered in the following figures are also marked: ○, figure 2; ×, figure 3; ∗, figure 4; □, figure 6(*a*); ◇, figure 6(*b*); +, figure 6(*c*); ▼, figure 6(*d*); △, figure 7; ■, figure 9.

pronounced maximum. Under these conditions the jet is narrow and typically breaks up into several small droplets. Further, they noticed a characteristic sound, the source of which they could not explain. At impact velocities just above the upper limit for high narrow jets they found wide jets rising to small heights only. From the tip of the wide jets only one large drop is separated. The jet height then increases gradually with the impact velocity. At impact velocities below the lower limit for the formation of high-rising narrow jets Hallett & Christensen (1984) observed non-breaking jets that were reported to rise up to a height of five drop diameters. The range of impact velocities yielding narrow high jets coincides with the regime of regular bubble entrainment (Rein 1993). The characteristic sound heard by Hallett & Christensen is thus likely to be caused by the entrained bubble.

The transition between the different characteristic impact scenarios described above is of fundamental fluid mechanical interest in that impacting drops provide an example of a free surface flow which is governed by inertial, gravitational, viscous and surface tension forces. In the transitional regime all of these forces play an important role. At present we are far from a detailed understanding of the physical mechanisms causing the transitions. Until now the phenomena occurring in the transitional regime between coalescence and splashing have almost always been studied on their own. In the following we will focus more closely on the transition between them. In particular, we will study how the characteristics of drop impact are changed when the impact conditions are gradually varied. Finally, a classification of the processes occurring in the transitional regime is provided by ordering the different phenomena according to the Weber number.

2. Experimental procedure

Drops were formed on the tip of a 20-gauge hypodermic needle that was mounted vertically. The needle was cut at right angles with respect to its axis. The open end was polished and its outer edge slightly rounded. In order to reduce disturbing effects caused by drop oscillations we carefully released small drops whose oscillations died away quickly. Small drops were produced by first letting liquid flow slowly from a reservoir through the hypodermic needle so that a pendant drop was formed. The growth of the drop was monitored using standard video equipment. When it had reached a certain size that was found to be suitable for a forced detachment from the needle the supply of liquid was stopped. The drop was then released by a weak impulse applied to the plastic tube connecting the needle with the liquid reservoir. The impulse was delivered by an iron cylinder accelerated electromagnetically against the tube. The diameter of the drops produced in this manner ranged from $D = 2.2$ to 2.5 mm. On impact the deviation from spherical shape measured by the relative difference ΔR (scaled by the drop radius) of the two half-axes of an ellipsoid representing the shape of the drop, was always less than 0.03. In many cases it was practically zero. The liquid of both the drop and the bulk was water. The receiving liquid was contained in a glass vessel of rectangular cross-section (83 mm × 83 mm) and of height 68 mm. The vessel was filled up to the brim in order to keep disturbances due to the meniscus small.

In order to visualize the flow of the drop liquid after impact we added potassium permanganate to the drop liquid using a mass fraction of 0.02. In contrast to many types of ink this hardly changed the surface tension. The surface tension was determined by the Wilhelmy plate method using a K10 tensiometer by Krüss. For water we obtained $\sigma_{H_2O} = 71.4 \times 10^{-3}\ \mathrm{N\,m^{-1}}$ while the surface tension of the solution was $\sigma_{sol} = 70.9 \times 10^{-3}\ \mathrm{N\,m^{-1}}$. The experiments were conducted at ambient temperature.

The field of view covered by the camera was chosen so that processes both above and below the liquid surface were observed. The optical axis was arranged to lie parallel to the surface. On the photographs the horizontal black line represents the surface of the receiving liquid. The impinging drops were illuminated by back-lighting using a light pulse generator (Stasicki, Hiller & Meier 1990). This pulse generator, which operates with an LED, is triggered by the camera. The duration of the light pulses was 10^{-6} s.

The photographs were taken with a LOCAM Model 50-0002 16 mm high-speed motion picture camera. The camera operates between 16 and 500 frames per second. We normally used the highest framing rate. In order to reach this rate before the drop impinges upon the liquid surface a time delay was arranged between the start of the camera and the release of the drop. Every 10^{-2} s the camera produces timing marks on the upper margin of the film. These are reproduced as white patches on the photographs shown in the next sections. A Kodak RAR 2494 film was used. More than 70 drop impacts were recorded with the high-speed camera. About half of these occurred under conditions characteristic of regular entrainment. The remaining impacts were equally divided between conditions corresponding to regions above and below the region of regular entrainment, respectively. In addition to these impacts with drops coloured with potassium permanganate, about 40 preliminary impacts were photographed with drops coloured with ink. Although the ink used affected the surface tension strongly, the characteristic features of the drop impacts were not changed. Except for figure 8 the results of the preliminary experiments will not be discussed.

The impact velocity u was regulated by changing the fall height h, i.e. the distance between the needle and the surface of the receiving liquid. During the evaluation it was

directly determined from the photographs. The range covered by the experiments was $u = 0.60$ to 2.61 m s^{-1}. Since the radius of the drops was approximately constant in all cases and $u^2 \sim h$, both the Weber and Froude number increased about linearly with the fall height. In a Weber versus Froude number diagram the data points are thus situated near a line of slope $Bo = We/Fr$, i.e. the Bond number, Bo, was constant. In the experiments the Weber and Froude numbers ranged from $We = 12$ to 223 and from $Fr = 15$ to 305, respectively. Since both the diameter of the drops and the impact velocity were directly taken from the photographs, the Weber and Froude numbers could be determined with an accuracy of at least 4%. The data points are distributed over the whole transitional regime, from the region of vortex ring formation to the region of splashing. The cases presented in photographic sequences in later sections are marked by different symbols in figure 1. In all sequences presented below the increase in time, Δt, between two successive photographs is approximately 2 ms and the scale is the same (the width of one frame corresponds to 12.8 mm). Different sequences can thus easily be compared. The exact difference in time between successive frames, Δt, is given in the figure captions.

3. Coalescence and vortex rings

Let us begin with coalescing drops that form vortex rings. Depending on the height from which the drops were released we obtained both well-developed vortex rings that moved far into the receiving liquid and rings that had a small propagation velocity only. For $We = 12$ and $Fr = 15$, which is well within the regime of coalescence, a vortex ring was formed that propagated far into the receiving liquid, eventually leaving the field of view. When $We = 26$ and $Fr = 31$ the propagation velocity of the vortex ring was very small and it came quickly to a rest. This is shown in figure 2. Here, the impinging drop was still slightly oscillating ($\Delta R \approx 0.03$). The first contact has formed in frame 2. In frame 3 coloured drop liquid can be seen below the original surface of the receiving liquid as a grey area. A crater, represented by a black region, can first be detected in frame 4. Drop liquid surrounds the crater, most of it being distributed beside and little beneath the crater. The drop liquid starts to roll up into a vortex ring in frame 5. When the crater recedes the vortex ring separates from the crater and begins to move slowly into the receiving liquid (frame 6 and thereafter). Then the vortex ring diffuses quickly into a blob of coloured drop liquid. Such blobs were previously reported by Cai (1989) and in a few cases by Rodriguez & Mesler (1988).

The penetration depth of a vortex ring depends on the phase of oscillation of the drop at impact. Most penetrating vortex rings are formed when a drop impinges with a prolate shape (Rodriguez & Mesler 1988). In the present case the shape of the drops on impact was not always discernible. However, in one case we were able to observe clearly that an impact of a prolate drop produced a well-penetrating vortex ring. The oscillations of drops that formed vortex rings had relative amplitudes of $\Delta R \approx 0.03$ at most (measured with respect to the drop radius). This is one order of magnitude smaller than in previous experiments (Chapman & Critchlow 1967; Rodriguez & Mesler 1988). Apparently, small oscillations like those present here may still be important.

A vortex ring carries away part of the energy of the impinging drop. This part was estimated using the vortex ring model by Taylor (1953) which provides a relation between the energy of a vortex ring and its propagation velocity, its diameter and the density of the fluid. The model was developed for vortex rings in infinitely extended fluids. However, for providing an estimate it may also be used here although a free

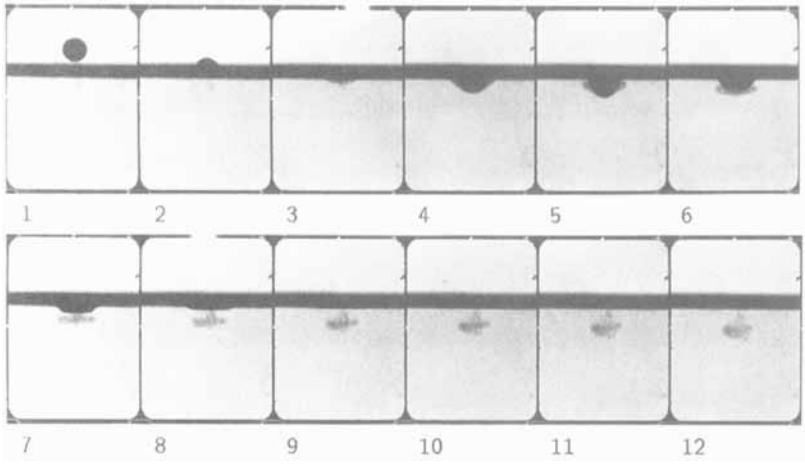

FIGURE 2. Impact of a water drop on a deep liquid resulting in the formation of a weak vortex ring. The impact conditions are: $We = 26$, $Fr = 31$, $u = 0.87$ m s^{-1} and $D = 2.48$ mm. The time difference between successive frames is $\Delta t = 2.08$ ms.

surface is present near the vortex ring. When the ring was well developed its energy amounted to more than one quarter of the impact energy. The energy of the weak ring that is shown in figure 2 was only approximately 5% of the impact energy.

The formation of a crater in the receiving liquid is connected with a redistribution of energy as well. When a vortex ring is weak more energy can be stored as potential energy of the crater, i.e. the crater may become larger. This was observed in our experiments where the crater reached a greater size with drop impacts that generated less-penetrating vortex rings. Similarly, Rodriguez & Mesler (1988) reported that a prolate drop (which generates a well-penetrating vortex ring) produced a narrow crater and an oblate drop a wide one. The wide crater was also deeper and thus larger. Both in our and in the latter case well-penetrating vortex rings, i.e. smaller craters, were obtained with impacts at Weber and Froude numbers that were smaller than those of impacts producing less-penetrating rings, i.e. larger craters. The Weber and Froude numbers provide a measure of the energies involved in an impact. At small Weber and Froude numbers an energy balance, in which the total energy of the drop is equated with the potential energy of the crater at its maximum size, normally yields smaller crater dimensions (cf. Prosperetti & Oğuz 1993). However, this dependence is not strong enough to explain the difference observed in the maximum crater size when vortex rings are formed. In the energy balance which yields good results in the region of regular entrainment of gas bubbles (Pumphrey & Elmore 1990) the contribution of the kinetic energy is normally assumed to be negligible when the crater has reached its maximum extension. In the region of coalescence, however, the kinetic energy of the vortex rings is no longer small. Furthermore, in addition to a primary ring which moves down into the liquid, complex vortex structures including secondary vortex rings are formed (Peck & Sigurdson 1994). The energy stored in these structures needs to be accounted for as well.

The formation of vortex rings is connected with the generation of vorticity. Recently, Cresswell & Morton (1995) proposed a mechanism of vorticity production which is restricted to low Weber numbers thus explaining the existence of a critical Weber number above which no vortex rings are formed. The mechanism is based on the condition of vanishing tangential stresses at a free surface. Immediately after impact

there is a cusp between the free surfaces of the drop and the receiving liquid. Here, surface tension forces are very large thus accelerating the surface normally to itself. In this manner streamlines become curved and a finite rate of strain is generated. In order to avoid tangential stresses at the free surface the surface is accelerated parallel to itself so that stresses are diminished and vorticity is produced. This mechanism works well at low impact velocities. With increasing impact velocities the mechanism competes with an effect known as surface destruction (Oğuz & Prosperetti 1989). Ahead of the cusp-like junction between the two liquids, the free surfaces approach each other so quickly that new contacts are formed thus causing a destruction of the free surface. According to Cresswell & Morton (1995) this phenomenon suppresses the formation of a vortex ring.

4. Transition to regular entrainment – change in crater dynamics

At Weber numbers just above the transition to jetting but below the lower boundary of regular entrainment of a gas bubble a drop impact results in the rise of a short thick central jet out of the crater. This case is presented in figure 3 which shows a drop impact with $We = 90$ and $Fr = 121$. Immediately after impact a wave swell is raised on the free surface of the receiving liquid at the circumference of the impact site (frame 2 etc.). The wave propagates radially outward as a capillary wave, carrying away some of the energy of the drop. At the same time a crater is formed that is larger than in the case of coalescence (cf. figure 2). In frames 6 and 7 coloured drop liquid can be seen beside the crater but under the present conditions a vortex ring is not formed. When the crater begins to collapse the drop liquid flows radially inward. Later, in addition to a flow up into a central jet the coloured drop liquid discloses a fluid motion that is directed downward. The tip of the jet can first be seen in frame 10 where the crater is practically gone. Its initial velocity is approximately a quarter of the impact velocity of the impinging drop but it quickly decreases. Both the maximum height and the thickness of the jet are comparable with the diameter of the impinging drop. The jet is thus not long enough to detach a tip droplet. When the central jet becomes smaller its diameter increases strongly at the foot of the jet. The coloured drop liquid seems to be only a little disturbed by the subsidence of the jet. The appearance of jets like this one serves as the criterion of the upper boundary of coalescence. Note that no secondary droplets are formed during this event. Neither does a droplet separate from the tip of the jet nor are there any droplets produced at the rim of the crater. This example of jetting could therefore as well be classified as coalescence.

The transition from vortex ring formation to jetting is accompanied by a change in the dynamics of the crater. In both cases the crater initially expands in all directions and it then assumes a shape that is approximately hemispherical. When a vortex ring is generated the expanding motion is first reversed at the bottom of the crater (cf. figure 2). During the contraction of the crater the main flow is directed upward. This is completely different in the jetting case. After the crater has reached its maximum depth fluid begins to flow radially inward from the sides while the lowest point of the crater remains at its position. Only later does the bottom of the crater begin to rise and a central jet is formed. There is thus a complex interaction between the crater dynamics, the disappearance of vortex rings and the initiation of jetting.

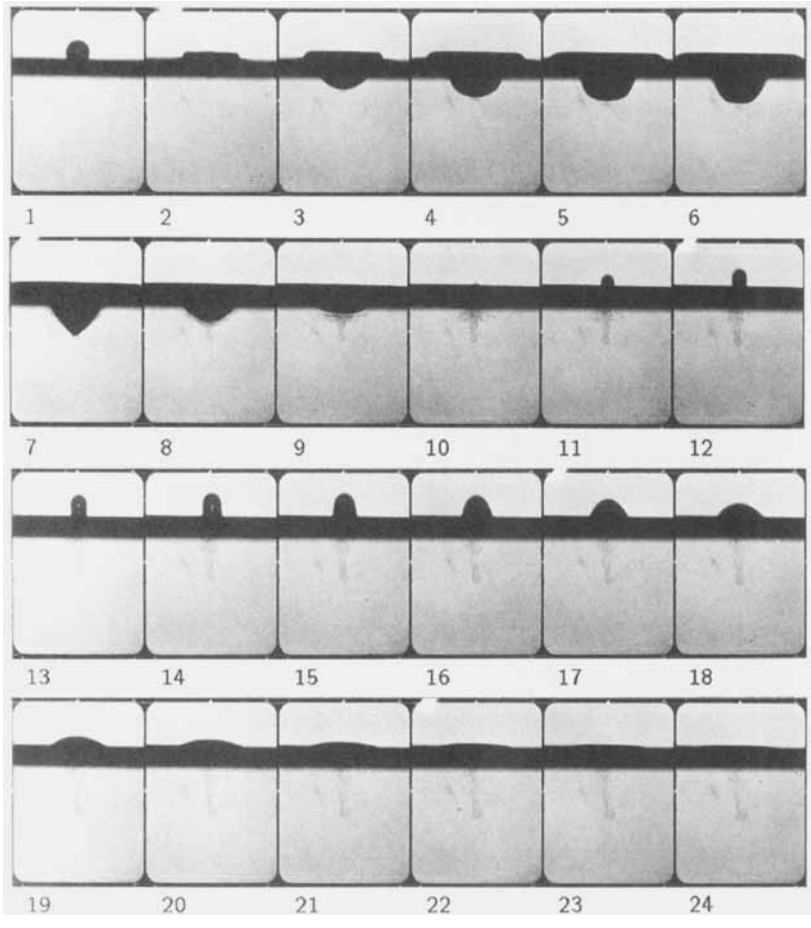

FIGURE 3. Formation of a short thick central jet after drop impact. The impact conditions are: $We = 90$, $Fr = 121$, $u = 1.66$ m s^{-1} and $D = 2.32$ mm. The time difference between successive frames is $\Delta t = 2.02$ ms.

5. Connection between bubble entrainment and the ejection of thin jets

Let us now turn to the region of regular entrainment of a gas bubble. Figure 4 presents an example that is well within this region ($We = 155$, $Fr = 213$). Immediately after impact a hemispherical crater is formed in the target liquid. At its floor drop liquid can be seen in frame 2. The size of the crater increases and its shape changes. Eventually, in frame 9, it assumes a conical shape with a small cylindrical stem at its bottom. Around the periphery of the crater a wave swell is formed that propagates radially outward as in the case considered in figure 3. When the crater relaxes a part of the cylindrical stem is pinched off and a bubble is entrained (frame 10). Only a very small time later a thin liquid jet is ejected out of the crater (frame 11). Tiny droplets having a radius of less than 0.1 mm precede the tip of the jet. In order to make these droplets clearly visible frame 11 is shown enlarged in figure 5. The velocity of the droplets is approximately twice the impact velocity. Without drag, they may thus rise up to four times the release height of the impinging drop, i.e. up to about 1 m. Presumably, it is the height reached by these droplets that was measured by Hallett & Christensen (1984) as the maximum jet height. The main body of the jet quickly reaches its maximum height (frame 17) and starts to thicken. At the same time the

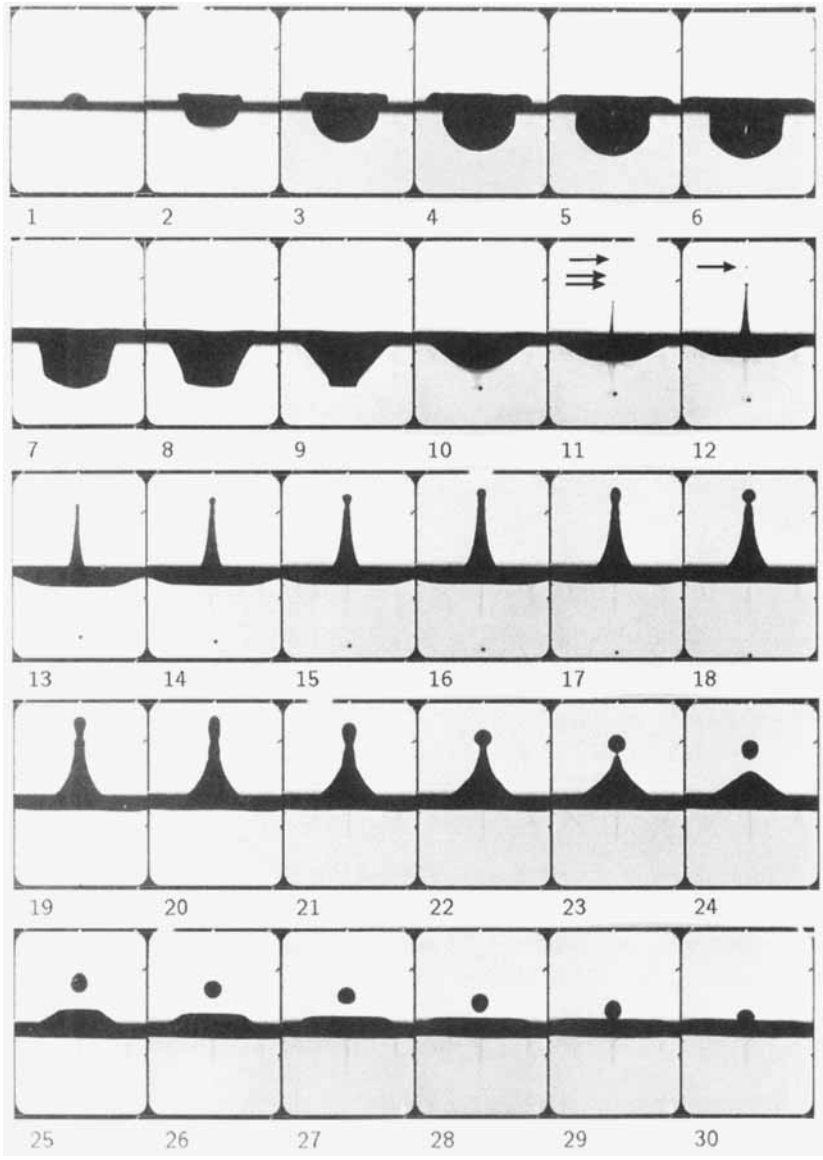

FIGURE 4. Drop impact on a deep liquid: connection between entrainment of a gas bubble and formation of a thin high-rising jet. Note the detachment of tiny droplets from the tip of the jet in frames 11 and 12. The impact conditions are: $We = 155$, $Fr = 213$, $u = 2.19$ m s^{-1} and $D = 2.30$ mm. The time difference between successive frames is $\Delta t = 2.14$ ms.

bubble moves downward and eventually leaves the section shown on the photographs (frame 19). On the axis of symmetry there is thus a flow of liquid up into the jet and also a small flow velocity downward. Some coloured liquid from the drop extends down to the bubble while other drop liquid is distributed around the receding crater. A vortex ring is not formed. The liquid jet becomes unstable and when its height decreases a big drop separates from its tip in frame 23. This drop oscillates strongly in its higher-order modes. When it touches the liquid surface it quietly disappears. On the photographs following this sequence the liquid surface is flat. Below the surface a blob of coloured liquid that may resemble a vortex ring could be seen.

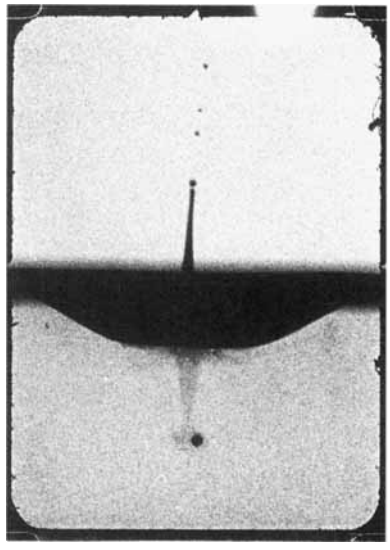

FIGURE 5. Enlargement of frame 11 of figure 4 showing tiny tip droplets moving ahead of the thin jet.

Further examples of drops impinging under conditions that traverse the whole region of regular entrainment are given in figure 6. The first sequence (figure 6*a*) shows an impact with $We = 102$ and $Fr = 120$ which is just above the lower threshold of regular entrainment. The next two cases lie well within the region of bubble formation (figure 6*b*: $We = 125$, $Fr = 177$ and figure 6*c*: $We = 164$, $Fr = 217$). The case shown in figure 6(*c*) is very close to the conditions of the last case (figure 4) and also to those of the one shown in the next figure (figure 7). Figure 6(*d*) is for conditions near the upper boundary of the region of regular entrainment ($We = 182$, $Fr = 249$). In these figures only a section of the full time series of the impact process is shown. In all cases it begins with a crater having a conical form and a thin jet appears in the third frame of each sequence of photographs. In figure 6(*a*) the thin jet is represented by tiny droplets only. In frame 4 of this sequence the tip of a thick central jet appears while the crater still recedes. The jet does not rise further but quickly disapears and all disturbances of the free surface quickly die away. In the next two cases (figure 6*b*, *c*) a short thin jet forms. Tiny droplets that precede its tip are again ejected with a high velocity. The jet then starts to thicken. The maximum height reached by the tip of the thick jet equals approximately the drop diameter. This is comparable with the case of jetting without entrainment shown in figure 3 but less than obtained under similar conditions (cf. figures 4 and 7). Note that a bubble was not entrained in figure 6(*b*). In the last sequence (figure 6*d*) the behaviour of the jet is similar to that observed in the cases shown in figures 4 and 7. It is interesting that the thin jet may be ejected obliquely (cf. figure 6*c*, *d*) but when it thickens it becomes normal to the undisturbed free surface of the receiving liquid. Finally, it should be mentioned that in none of the cases shown in figure 6 does a large tip drop separate from the central jet. The only droplets ejected are the tiny droplets that appear first.

In some cases drop impacts occurring under conditions characteristic of regular entrainment resulted in atypical flow patterns. In particular, a bubble was not entrained in about every eighth impact. An example is shown in figure 7. The Weber and Froude numbers are $We = 161$ and $Fr = 220$. This is very close to the cases shown in figures 4 and 6(*c*). The sequence begins again at a time when the crater has assumed

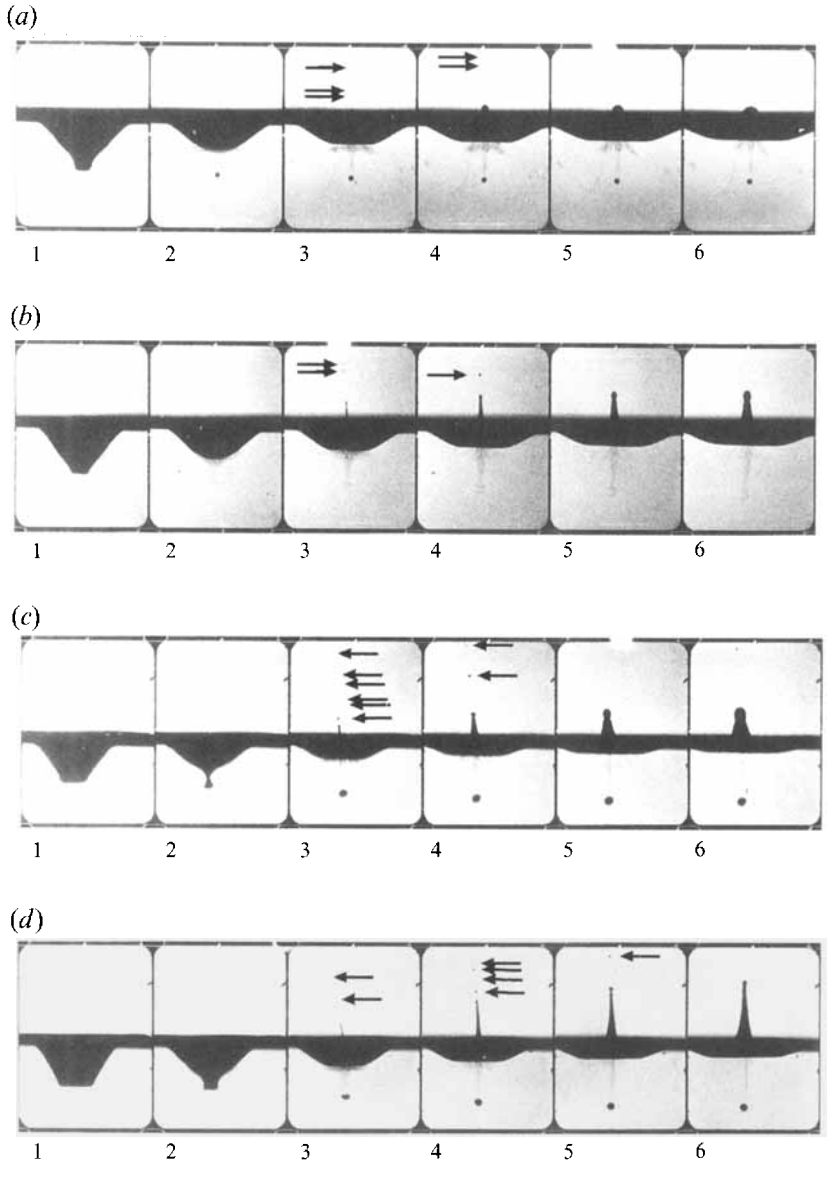

FIGURE 6. Comparison of drop impacts taking place under different conditions that are all within the region of regular entrainment: entrainment of a gas bubble, ejection of tiny droplets, formation of a thin jet and thickening of the jet. All photographic sequences begin shortly before the crater bottom reverses its motion. (*a*) $We = 102$, $Fr = 120$, $u = 1.71$ m s^{-1}, $D = 2.48$ mm and $\Delta t = 1.96$ ms; (*b*) $We = 125$, $Fr = 177$, $u = 1.98$ m s^{-1}, $D = 2.26$ mm and $\Delta t = 1.95$ ms; (*c*) $We = 164$, $Fr = 217$, $u = 2.23$ m s^{-1}, $D = 2.34$ mm and $\Delta t = 1.95$ ms; (*d*) $We = 182$, $Fr = 249$, $u = 2.37$ m s^{-1}, $D = 2.30$ mm and $\Delta t = 1.93$ ms.

a conical shape with a small cylindrical stem at its bottom. Up to this stage the process of crater formation proceeded in the usual manner (cf. figure 4). This time, however, a bubble is not pinched off. However, tiny droplets and a thin jet are again ejected out of the collapsing crater with high speed. Later when the jet thickens more disturbances are present on the jet than usually, as can already be seen in frame 5. This causes a Rayleigh breakup of the whole jet leading to the separation of two large and one small

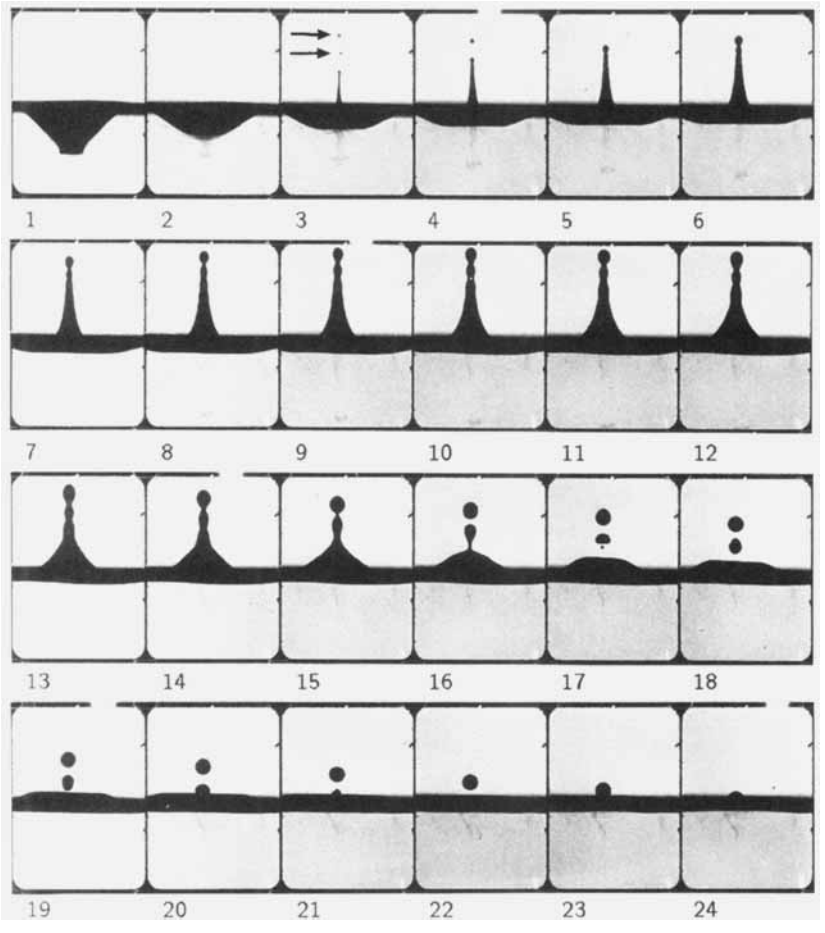

FIGURE 7. Drop impact occurring under conditions characteristic of regular entrainment. The sequence begins shortly before the crater bottom reverses its motion. Note that a thin jet is ejected upward but a bubble is not pinched off from the collapsing crater. The impact conditions are: $We = 161$, $Fr = 220$, $u = 2.23$ m s^{-1} and $D = 2.30$ mm. The time difference between successive frames is $\Delta t = 1.93$ ms.

satellite droplet (frame 17) while the jet subsides. Note that even at Weber numbers slightly above the upper boundary of regular entrainment normally only one tip droplet separates from the jet. Except for these features the whole process proceeded in the usual way, in particular very much as the one shown in figure 5.

5.1. *Entrainment of gas bubbles*

The entrainment of a bubble is caused by the dynamics of the crater during its collapse. At Weber numbers above the threshold for jetting the collapse begins at its sides. This leads to an intermediate crater shape that is close to conical. Under conditions of regular entrainment the different times at which the sides and the bottom of the crater begin to reverse their motion eventually cause the crater to assume a shape that is really conical. At its bottom a small cylindrical stem is formed. During this phase the depth of the crater does not change. Shortly before the stem is pinched off its bottom is accelerated downward (cf. figure 6*c*, frames 1 and 2). The newly formed bubble then moves down into the bulk liquid. Finally, after a time that is long compared with the

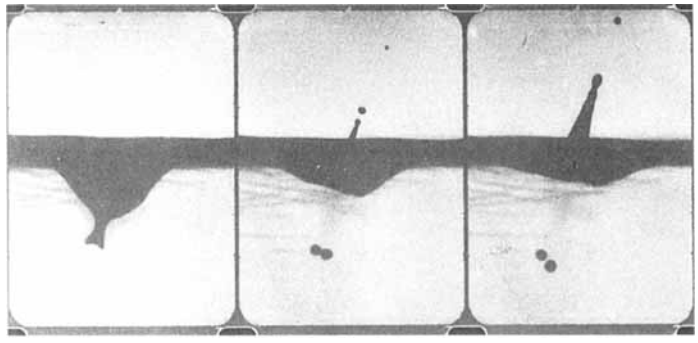

FIGURE 8. Drop impact onto a wavy liquid surface causing a simultaneous entrainment of two bubbles. Only the formation of the bubbles and the ejection of a thin jet are shown. The impact conditions are: $We = 115$, $Fr = 58$, $u = 1.35$ m s^{-1} and $D = 3.18$ mm. The time difference between successive frames is $\Delta t = 2.2$ ms.

time scales of crater collapse and jetting, buoyancy forces become dominant and the bubble rises to the surface where it stays for a while and then bursts. At the transition into the region of regular entrainment the dynamics of the crater change only slightly. In particular, at the bottom of the crater a small disturbance resembling a cylindrical stem can already be found for drop impacts in the jetting regime but below the region of regular entrainment (cf. figure 3, frame 7).

A bubble was normally but not always formed under impact conditions of regular entrainment. The size of entrained bubbles did not correlate with the impact conditions, i.e. with the Weber and Froude numbers. Its radius varied by a factor of about two. In two cases, however, only a tiny bubble was separated from the crater. It may well be that the surface of the receiving liquid was sometimes slightly contaminated by a surfactant. The presence of surfactants can cause the observed irregularities in bubble size, including a total suppression of bubble entrainment. On the other hand the crater collapse always proceeded in the usual way. A cylindrical stem can still be seen to form in the case considered in figure 7 (first frame) although a bubble does not appear. The process of stem pinch-off, which proceeds on very small time scales, is caused by a radial focusing of the flow (see §5.2). It is not clear whether surfactants will influence the flow during this short stage. Furthermore, when surfactants play a role one would expect the crater collapse to proceed in a manner characteristic of impacts under conditions corresponding to a Weber number calculated with a reduced surface tension. The present irregularities in bubble entrainment may therefore also be caused by other disturbances although in the relevant cases disturbances of the impact process, such as drop oscillations, could not be discerned.

In practical situations the surface of the receiving liquid is not still. In one case we accidentally photographed a drop impinging onto a wavy surface, i.e. impinging obliquely. The waves were created by a preceding impact. The fluid flow is no longer axially symmetric. This resulted in a distortion in the shape of the crater which upon collapse pinched off two bubbles. Further, both the thin and the thick jet were ejected obliquely. This is shown in figure 8. The sequence stems from a preliminary experiment in which ink was used to colour the drop liquid. Its surface tension was $\sigma = 50.4 \times 10^{-3}$ N m^{-1}. The corresponding Weber and Froude numbers are $We = 115$ and $Fr = 58$. Here, the Weber number was calculated with the reduced surface tension of the drop liquid. A simultaneous entrainment of two or possibly more bubbles by oblique impacts may have a direct impact on the spectrum of underwater noise of rain

because the radiation of a system of two oscillating bubbles will differ from that of one bubble. The spectrum which has a characteristic peak at 14 kHz broadens under windy conditions (Prosperetti *et al.* 1989). The presence of wind causes drops to impinge obliquely. Following Medwin, Kurgan & Nystuen (1990) this reduces the probability of bubble entrainment and, thus, the contribution of bubble noise to the total spectrum is diminished. A change in the radiation pattern due to the entrainment of pairs of bubbles may also contribute to a broader spectrum.

5.2. *Thin high-rising jets*

In the region of regular entrainment drop impacts always caused the ejection of a thin liquid jet out of the crater. The initial velocity of the jet is clearly greater than the impact velocity. The thin jet breaks up quickly and several tiny droplets are formed. The breakup of the jet may occur within the cavity so that only droplets but not the thin jet rise above the surface of the receiving liquid. The initial velocity of the first small droplets that precede the jet may be up to three times as large as the velocity of the jet. It should be emphasized that the ejection of a thin jet happened at each impact within the region of regular entrainment. In contrast to this a bubble was generally but not always formed. The appearance of a thin jet may thus be considered to be more characteristic of the region of regular entrainment than the formation of a bubble.

The ejection of little droplets or of a thin jet has not been previously reported in connection with regular entrainment of bubbles. Drop impacts causing regular entrainment that are shown in other works usually occurred at relatively small Weber and Froude numbers, i.e. the impacts took place under conditions not too far from the lower boundary of regular entrainment in a Weber versus Froude number diagram. In such cases a thin jet may not rise above the rim of the crater and only several tiny droplets appear prior to a thick jet. In order to resolve these fast-moving droplets very short exposure times are necessary. When using high-speed cameras with constant back-lighting or taking still pictures with photographic flashes exposure times may well be greater than in the present case.

Thin high-rising jets with similar properties to the ones observed here were detected by Hobbs & Osheroff (1967) during the splash of drops on shallow liquid layers of certain depths. Highest jets occurred for depths at which the crater at its maximum extension was about to touch the bottom of the liquid layer (Macklin & Hobbs 1969). At smaller depths the maximum jet height decreased abruptly. Shin & McMahon (1990) found that the collapse of the crater is similar to a crater collapse leading to the entrainment of a bubble in deep liquids, if the depth of the layer is such that the crater at its maximum size just touches the bottom. In particular, a cylindrical stem is formed at the bottom of the crater. As in the case of regular bubble entrainment the upward motion of the cylindrical stem is delayed. Here, the closeness of the solid wall prevents flow into the crater from below. When the solid wall was replaced by a sponge, thus enabling an upward flow into the crater, the jetting motion was mostly suppressed. Shin & McMahon (1990) proposed that the formation of the cylindrical stem is necessary for the ejection of thin jets in shallow liquid splashes. At the stem a greater curvature causes greater surface tension forces and, thus, a higher pressure difference across the liquid surface. This pressure difference, which is enhanced by hydrostatic forces, was assumed to be responsible for the formation of high-rising thin jets in shallow liquid splashes.

After drop impacts in both deep and shallow liquids, the velocity has a strong component in the radial direction toward the axis of symmetry shortly before a thin jet

is formed. With decreasing cavity radius the liquid is accelerated inward. This is known as radial focusing. Eventually the fluid escapes in the axial direction, forming a thin high-speed jet moving upward. In deep liquids there is also a slow flow directed downward. In this manner momentum is conserved. These processes are similar to the Munroe effect which causes jetting in shaped charges. This was pointed out by MacIntyre (1968) in connection with jetting after the burst of a bubble at a liquid surface. In shaped charges a hollow of, for example, conical shape is lined by a metal. Explosives accelerate the liner inward and upon collision with the opposing liner both a thin high-speed jet, which is directed out of the hollow, and a thick slow jet, which is directed backward, are formed. These flows can be well modelled by an incompressible approach based on the principle of conservation of momentum (Birkhoff *et al.* 1948). However, compressibility also plays a role. The forward-facing thin jet can only be formed if the angle between the colliding surfaces exceeds a certain threshold which is connected with the maximum angle of deflection of attached oblique shock waves (Walsh, Shreffler & Willig 1953). Related issues were analysed by Rein (1995*b*) for the case of high-speed collisions between two liquids. A high-speed impact between liquids is also present when the liquid closes above the bubble during crater collapse. The impact happens along a line of contact on the axis of symmetry. After impact a shock wave propagates into the liquid. Initially the shock adheres to the ends of the line of contact thus enclosing a high-pressure region. With increasing vertex angle of the collapsing crater the conditions for the shock to remain attached to the end of the contact line break down. The shock then moves ahead of the end of the contact line and axial jetting of the liquid out of the high-pressure region begins. In the case of bubble entrapment this happens very shortly after the first contact is formed. The high-pressure region will therefore be small and on the whole compressibility effects are of minor importance. However, the ejection of tiny droplets with high velocities that exceed the velocity of the thin jet may well be due to high pressures in the shocked region.

The mechanisms of jetting discussed in the last paragraph are largely independent of properties such as surface tension and viscosity. This is in agreement with the findings of Shin & McMahon (1990) who observed that a change of these parameters had little influence on jet formation after drop impact on shallow liquid layers. The maximum size of the crater depends mainly on the Froude number (Prosperetti & Oğuz 1993). The Weber number is of minor importance. When the crater at its maximum size just touches the bottom of a shallow liquid layer the radial flow causing the collapse of the crater is induced by the presence of the solid wall below the crater. This is different for drops falling into deep liquids. Here, surface tension forces have an important influence on the dynamics of crater collapse. A variation in surface tension, e.g. by addition of surfactants, changes the Weber number and can suppress the mechanism causing the entrainment of a bubble (Pumphrey & Crum 1988) and, possibly, also the ejection of a thin jet.

6. Thick jets and tip droplets

Drop impacts occurring for Weber and Froude numbers that lie just above the region of regular entrainment are in many respects similar to drop impacts causing jetting below this region. The characteristics of such impacts are shown in figure 9 which was obtained for $We = 219$ and $Fr = 305$. The sequence starts again at the moment when the crater has assumed a form that is close to conical. However, an exactly conical form no longer appeared. After impact a thick wave swell propagating

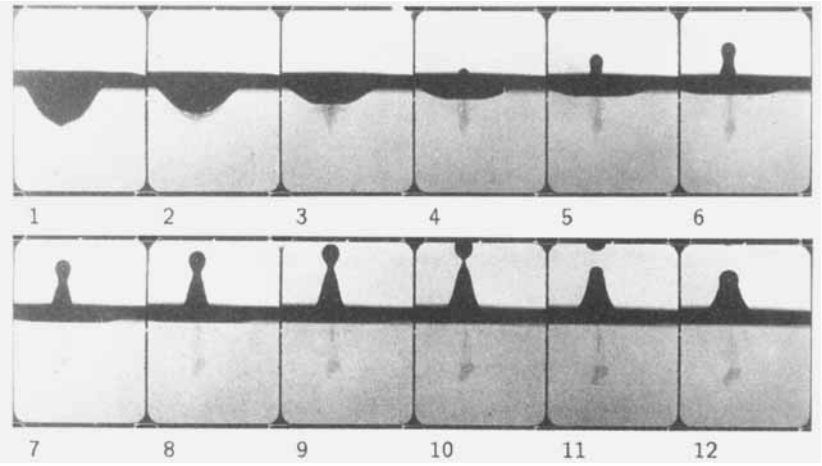

FIGURE 9. Drop impact occurring under conditions that are above the region of regular entrainment: formation of a thick central jet and detachment of a big tip drop. The sequence begins at the moment when the base of the crater reverses its motion. The impact conditions are: $We = 219$, $Fr = 305$, $u = 2.61$ m s^{-1} and $D = 2.28$ mm. The time difference between successive frames is $\Delta t = 1.92$ ms.

radially outward is formed at the rim of the growing crater. When the crater has reached its greatest depth the collapse again begins from the sides while the deepest point of the crater remains fixed for a short moment. Eventually the crater assumes an intermediate shape which is close to conical and shows a small bump at its bottom which is reminiscent of the cylindrical stem appearing in the region of regular entrainment (see the first frame of figure 9). The effect of radial focusing is weakened. Then the bottom of the crater begins to move upward and shortly thereafter a thick jet rises out of the crater (frame 4). The velocity of the jet is small, typically about a quarter of the impact velocity. This is similar to the case of jetting at a Weber number that is below the lower boundary of regular entrainment (cf. figure 3) but in the present case the velocity of the jet decreases more slowly and the jet rises to a greater height so that the jet becomes long enough for a droplet to separate from its tip (frame 10). The detached tip droplet rises further while the jet quietly subsides into the bulk liquid. The tip droplet later leaves the field of view (frame 12). From the time when it reappears its maximum height can be estimated to equal about 12 mm. This is comparable with data reported by Hallett & Christensen (1984) but it is clearly greater than the maximum height reached by the jet of the case shown in figure 3 as is appropriate at higher Weber numbers, i.e. higher impact energies. On the other hand the tiny droplets which are typically ejected under conditions characteristic of regular entrainment reach much greater heights. The big tip droplet is the only secondary droplet produced under these conditions. Close to the boundary of regular entrainment only one big tip droplet is pinched off. At higher impact energies more than one droplet may detach from the jet.

7. Wave swells, crowns and splashing

In all cases a wave swell was raised around the impact site of the drop. Sometimes it was not visible on the photographs since its height was not big enough for its apex to rise above the meniscus. Typically, this was the case for coalescing drops and for impacts corresponding with the lower part of the region of regular entrainment. Under

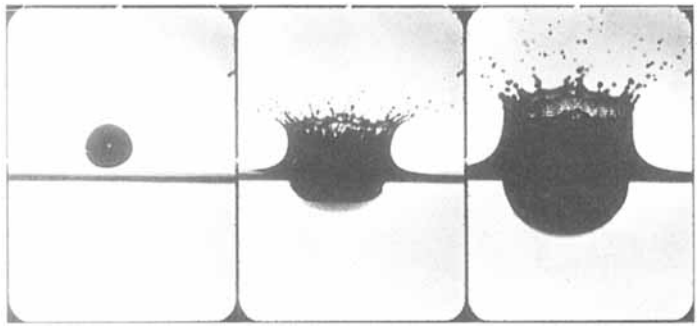

FIGURE 10. Splash: ejection of a thin cylindrical liquid sheet and generation of many splash droplets. The impact conditions are: $We \approx 1750$, $Fr \approx 500$, $u \approx 5$ m s^{-1} and $D \approx 5$ mm. Note that the scale of the photographs has been changed. Here, the width of one frame corresponds to 24.4 mm. The time difference between successive frames is $\Delta t \approx 2$ ms.

these conditions the wave becomes visible when the optical axis is slightly inclined to the surface of the receiving liquid so that the view is somewhat from above. The wave swell is formed shortly after the base of the drop reaches the undisturbed level of the receiving liquid. It then propagates radially outward. Initially it remains attached to the rim of the growing crater. Later when the expansion of the crater slows down, i.e. before the crater reaches its maximum size, the wave separates from the rim and continues to move radially outward.

The wave swell needs to be distinguished from a thin cylindrical liquid film, the so-called crown, which may also be ejected upward at the periphery of impinging drops. The upper edge of the liquid film becomes unstable and small jets emanate from its rim. These disintegrate into many secondary droplets. The instability of the cylindrical film provides the main mechanism of the production of splash droplets. The appearance of a crown is thus characteristic of splashing in its fully developed form.

A crown was never found under impact conditions considered up to now. We therefore greatly increased the impact energy by both doubling the drop diameter and releasing the drop from a greater height. At Weber and Froude numbers of $We \approx 1750$ and $Fr \approx 500$, respectively, a thin cylindrical liquid film was ejected out of the liquid around the impacting drop with velocities that are comparable with the impact velocity. This can be seen in figure 10. Only the first frames are shown because the splash expands quickly over an area that is greater than the field of view. Furthermore, in this case the glass vessel was no longer large compared with the disturbances produced by the impact. Under the present conditions the liquid sheet was about to bend inward and close above the crater forming a big bubble on the surface of the receiving liquid. A crown can be formed at smaller Weber numbers. Hallett & Christensen (1984) reported that they observed crown formation at Weber numbers as small as $We = 180$. Detailed data are not provided so that this number is of little use. Complete impact conditions for crown formation at relatively small Weber numbers are, e.g. $We \approx 230$ and $Fr \approx 70$ (Cai 1989) and $We \approx 470$ and $Fr \approx 100$ (Pumphrey, Crum & Bjørnø 1989). The former Weber number is only slightly greater than that of our example for the formation of a thick jet above the region of regular entrainment in which a crown did not form ($We = 219$ and $Fr = 305$, cf. figure 9). Note that the Froude numbers are different. When a crown forms, a thin sheet of liquid is ejected upward at the periphery of the drop immediately after impact. This can well be seen, for example, in photographs of Wilkens (cf. Rein 1993). With increasing time the crown thickens and changes into a wave swell. The wave swell then separates from the

rim of the expanding crater and propagates radially outward as discussed above. The subsequent crater collapse proceeds in the usual way producing a thick jet from which one or more tip droplets separate.

A crown appears only at large Weber numbers. This indicates that there may exist an additional boundary beyond which crown formation occurs although such a boundary, e.g. in terms of a critical Weber number, at which this transition takes place has never been reported. However, it is also possible that a cylindrical liquid film is always ejected after impact. At small Weber numbers it may be so small that it remains hidden under the approaching drop and merges quickly with the rising wave swell so that it cannot normally be detected. A different explanation is that the ejected thin sheet of liquid adheres to the surface of the drop at small Weber numbers. It then begins to wrap around the drop and can hardly be distinguished from its surface. This is corroborated by observations of Cresswell & Morton (1992, 1995) who noticed that immediately after impact the contact line between the two liquids rises up the surface of the drop. The transition to crown formation may then be similar to the case of smooth spheres falling into a liquid (Worthington 1900). At small impact velocities a smooth sphere becomes fully enclosed by the receiving liquid. When the sphere is released from greater heights the liquid film separates from its surface thus initiating splashing.

Finally, it is suggested that the thin cylindrical liquid film ejected upward belongs to a class of kinematic discontinuities that are connected with a sink. Discontinuities of this type were recently introduced by Yarin & Weiss (1995). These authors found that the formation of a kinematic discontinuity with a sink is responsible for the transition to splashing in the case of drops impinging consecutively onto the same site on a solid wall. Physically the sink is realized by the uprising liquid sheet of the crown. In the case of single drops impinging on deep liquid layers the receiving liquid is instantaneously displaced after impact. This situation can be compared with the piston problem of gas dynamics where a shock forms when a piston is suddenly advanced with a finite velocity into a tube. There the shock separates immediately from the piston and propagates into the tube. However, if the shock were connected with a sink it need not necessarily separate from the piston. In the present case the ejected liquid film can therefore remain attached to the advancing contact circle between the drop and the undisturbed level of the receiving liquid. Note that this may happen both when the liquid film adheres to the surface of the drop and when it separates from it, eventually forming a crown.

8. Conclusions

The characteristics of different flows that appear in the transitional regime between coalescing and splashing drops, and possible mechanisms causing these flows have been discussed in detail considering the normal impact of water drops on a plane water surface. The discussion was based on high-speed photographs of drop impacts occurring under different conditions. Several new features were found. In particular, these include a change in the dynamics of the crater collapse when a vortex ring ceases to appear. In the region of vortex ring formation the expanding motion of the crater is first reversed at its bottom by a flow directed vertically upward. Here, a significant fraction of the energy of the impinging drop can be transformed into kinetic energy of the vortex ring. In the region of jetting most of the impact energy is used up in forming the crater. The subsequent crater collapse then begins at the sides causing a radial focusing of the flow. Furthermore, we have shown that drop impacts in the region of

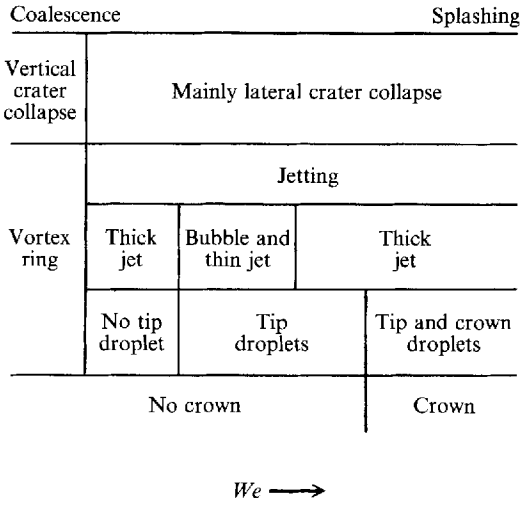

FIGURE 11. Transition from coalescence to splashing: characteristics of different flow patterns ordered according to the Weber number.

regular entrainment are always connected with the ejection of a thin high-rising liquid jet out of the centre of the collapsing crater. In contrast to this the entrainment of a bubble may be suppressed by a small disturbance. In addition, it was proposed that the thin cylindrical liquid sheet that may be ejected out of the receiving liquid at the periphery of the impinging drop belongs to a class of kinematic discontinuities with a sink that was recently introduced by Yarin & Weiss (1995) in connection with splashing on solid walls. The sheet of liquid becomes unstable, disintegrates and develops into the well-known crown. The instability of the liquid sheet is the main mechanism for the generation of secondary droplets by drop impact. Splashing is thus fully developed only when a crown is formed.

In addition to a description of the characteristics of different flow patterns we can now provide a comprehensive classification of the processes occurring in the transitional regime. The main parameter governing the transition is the ratio of the kinetic to the surface energy of the impinging drop, i.e. the Weber number. The Froude number, which measures the importance of the potential energy of the impact crater, is also of some influence. In a Weber versus Froude number diagram regions can be distinguished that correspond to different fluid motions. The boundaries of the region of regular entrainment were carefully determined by Pumphrey *et al.* (1989). But other boundaries, such as the conditions for the onset of crown formation, still need to be found or to be determined more exactly. Purpose of the present work was to classify and discuss the main characteristics of the flows in the transitional regime. These are ordered according to the Weber number in figure 11. Numerical values have not been specified since Weber numbers characteristic of boundaries between different phenomena depend on the Froude number. Moreover, they are often not known exactly. Below a critical Weber number an impinging drop will coalesce and form a vortex ring. Above this Weber number a central jet rises out of the crater and a vortex ring no longer appears. The case of jetting is divided into several regions. At small Weber numbers a very short thick jet appears. Secondary droplets are not formed. Then the region of regular entrainment follows. Here, besides the formation of a gas bubble, a thin high-rising jet is ejected out of the crater. From the tip of the thin jet little secondary droplets are detached. At Weber numbers above the region of regular

entrainment the central jet is again thick. It now rises to greater heights and one or more big droplets break off from the tip. Up to this stage secondary droplets are due to a disintegration of the central jet only. Therefore only a few tip droplets are generated. Vigorous splashing causing the formation of many secondary droplets that are shed from the rim of a cylindrical liquid sheet appears only when the Weber number is further increased. At even greater Weber numbers additional flow patterns may appear. However, these are not the subject of this investigation.

The present experiments and most previous ones reported in the literature were conducted with water. Exceptions are, for example, qualitative experiments by Thompson & Newall (1885). Prosperetti & Oğuz (1993) presented some detailed data of the upper and lower boundaries of the region of regular entrainment obtained with liquids of various viscosities. These data clearly indicate that the importance of the viscosity reaches far into the region of jetting. In order to obtain a deeper understanding of the transitional regime between coalescing and splashing drops it will be necessary to investigate the influence on the resulting flow patterns of both viscosity and surface tension more closely. Then an additional non-dimensional number like the capillary or the Reynolds number will be needed to describe the transition processes.

The photographs were taken by Mr P. Koperski whose help is gratefully acknowledged. This work was partially supported by the Deutsche Forschungsgemeinschaft.

REFERENCES

BIRKHOFF, G., MACDOUGALL, D. P., PUGH, E. M. & TAYLOR, G. I. 1948 Explosives with lined cavities. *J. Appl. Phys.* **19**, 563–582.

CAI, Y. K. 1989 Phenomena of a liquid drop falling to a liquid surface. *Exps. Fluids* **7**, 388–394.

CHAPMAN, D. S. & CRITCHLOW, P. R. 1967 Formation of vortex rings from falling drops. *J. Fluid Mech.* **29**, 177–185.

CRESSWELL, R. W. & MORTON, B. R. 1992 Raindrops in the sea II – Experimental studies of vortex ring generation. In *Proc. 11th Australasian Fluid Mech. Conf., University of Tasmania, Hobart* (ed. M. R. Davis & G. J. Walker), pp. 615–618.

CRESSWELL, R. W. & MORTON, B. R. 1995 Drop-formed vortex rings – The generation of vorticity. *Phys. Fluids* **7**, 1363–1370.

HALLETT, J. & CHRISTENSEN, L. 1984 Splash and penetration of drops in water. *J. Recherches Atmos.* **18**, 225–242.

HOBBS, P. V. & OSHEROFF, T. 1967 Splashing of drops on shallow liquids. *Science* **158**, 1184–1186.

HSIAO, M., LICHTER, S. & QUINTERO, L. G. 1988 The critical Weber number for vortex and jet formation for drops impinging on a liquid pool. *Phys. Fluids* **31**, 3560–3562.

MACINTYRE, F. 1968 Bubbles: a boundary-layer 'microtome' for micron-thick samples of a liquid surface. *J. Phys. Chem.* **72**, 589–592.

MACKLIN, W. C. & HOBBS, P. V. 1969 Subsurface phenomena and the splashing of drops on shallow liquids. *Science* **166**, 107–108.

MEDWIN, H., KURGAN, A. & NYSTUEN, J. A. 1990 Impact and bubble sound from raindrops at normal and oblique incidence. *J. Acoust. Soc. Am.* **88**, 413–418.

OĞUZ, H. N. & PROSPERETTI, A. 1989 Surface-tension effects in the contact of liquid surfaces. *J. Fluid Mech.* **203**, 149–171.

OĞUZ, H. N. & PROSPERETTI, A. 1990 Bubble entrainment by the impact of drops on liquid surfaces. *J. Fluid Mech.* **219**, 143–179.

PECK, B. & SIGURDSON, L. 1994 The three-dimensional vortex structure of an impacting water drop. *Phys. Fluids* **6**, 564–576.

PROSPERETTI, A. & OĞUZ, H. N. 1993 The impact of drops on liquid surfaces and the underwater noise of rain. *Ann. Rev. Fluid Mech.* **25**, 577–602.

PROSPERETTI, A., PUMPHREY, H. C. & CRUM, L. A. 1989 The underwater noise of rain. *J. Geophys. Res.* **94**, 3255–3259.

PUMPHREY, H. C. & CRUM, L. A. 1988 Acoustic emissions associated with drop impacts. In *Sea Surface Sound* (ed. B. R. Kerman), pp. 463–483. Kluwer.

PUMPHREY, H. C., CRUM, L. A. & BJØRNØ, L. 1989 Underwater sound produced by individual drop impacts and rainfall. *J. Acoust. Soc. Am.* **85**, 1518–1526.

PUMPHREY, H. C. & ELMORE, P. A. 1990 The entrainment of bubbles by drop impacts. *J. Fluid Mech.* **220**, 539–567.

PUMPHREY, H. C. & WALTON, A. J. 1988 Experimental study of the sound emitted by water drops impacting on a water surface. *Eur. J. Phys.* **9**, 225–231.

REIN, M. 1993 Phenomena of liquid drop impact on solid and liquid surfaces. *Fluid Dyn. Res.* **12**, 61–93.

REIN, M. 1995*a* Wave phenomena during droplet impact. In *IUTAM Symp. on Waves in Liquid/Gas and Liquid/Vapor Two-Phase Systems* (ed. S. Morioka & L. van Wijngaarden), pp. 171–190. Kluwer.

REIN, M. 1995*b* Maximum pressures during hypervelocity liquid–liquid impact. In *IUTAM Symp. on Waves in Liquid/Gas and Liquid/Vapor Two-Phase Systems* (ed. S. Morioka & L. van Wijngaarden), pp. 191–200. Kluwer.

RODRIGUEZ, F. & MESLER, R. 1985 Some drops don't splash. *J. Colloid Interface Sci.* **106**, 347–352.

RODRIGUEZ, F. & MESLER, R. 1988 The penetration of drop-formed vortex rings into pools of liquid. *J. Colloid Interface Sci.* **121**, 121–129.

SHIN, J. & MCMAHON, T. A. 1990 The tuning of a splash. *Phys. Fluids* A **2**, 1312–1317.

STASICKI, B., HILLER, W. J. & MEIER, G. E. A. 1990 Light pulse generator for high speed photography using semiconductor devices as a light source. *Opt. Engng* **29**, 821–827.

TAYLOR, G. I. 1953 Formation of a vortex ring by giving an impulse to a circular disk and then dissolving it away. *J. Appl. Phys.* **24**, 104–105.

THOMPSON, J. J. & NEWALL, H. F. 1885 On the formation of vortex rings by drops falling into liquids, and some allied phenomena. *Proc. R. Soc. Lond.* **39**, 417–436.

WALSH, J. M., SHREFFLER, R. G. & WILLIG, F. J. 1953 Limiting conditions for jet formation in high velocity collisions. *J. Appl. Phys.* **24**, 349–359.

WORTHINGTON, A. M. 1897 Impact with a liquid surface, studied by the aid of instantaneous photography. *Phil. Trans. R. Soc. Lond.* A **189**, 137–148.

WORTHINGTON, A. M. 1900 Impact with a liquid surface studied by the aid of instantaneous photography. Paper II. *Phil. Trans. R. Soc. Lond.* A **194**, 175–199.

YARIN, A. L. & WEISS, D. A. 1995 Impact of drops on solid surfaces: self-similar capillary waves and splashing as a new type of kinematic discontinuity. *J. Fluid Mech.* **283**, 141–173.